TISSUE ENGINEERING: Part A
Volume 24, Numbers 17 and 18, 2018

DOI: 10.1089/ten.tea.2017.0448

termis
Tissue Engineering
& Regenerative Medicine
International Society

ORIGINAL ARTICLE

Human Osteoblast-Derived Extracellular Matrix with High Homology to Bone Proteome Is Osteopromotive

Marta Baroncelli, MSc,[1] Bram C.J van der Eerden, PhD,[1] Siddharth Chatterji, MSc,[1] Enrique Rull Trinidad, MSc,[2] Yik Y. Kan, MSc,[1] Marijke Koedam, MSc,[1] Ingmar A.J van Hengel, MSc,[3] Rodrigo D.A.M. Alves, PhD,[1] Lidy E. Fratila-Apachitei, PhD,[3] Jeroen A.A. Demmers, PhD,[4] Jeroen van de Peppel, PhD,[1] and Johannes P.T.M. van Leeuwen, PhD[1]

Efficient osteogenic differentiation of mesenchymal stromal cells (MSCs) is crucial to accelerate bone formation. In this context, the use of extracellular matrix (ECM) as natural 3D framework mimicking *in vivo* tissue architecture is of interest. The aim of this study was to generate a devitalized human osteogenic MSC-derived ECM and to investigate its impact on MSC osteogenic differentiation to improve MSC properties in bone regeneration. The devitalized ECM significantly enhanced MSC adhesion and proliferation. Osteogenic differentiation and mineralization of MSCs on the ECM were quicker than in standard conditions. The presence of ECM promoted *in vivo* bone formation by MSCs in a mouse model of ectopic calcification. We analyzed the ECM composition by mass spectrometry, detecting 846 proteins. Of these, 473 proteins were shared with the human bone proteome we previously described, demonstrating high homology to an *in vivo* microenvironment. Bioinformatic analysis of the 846 proteins showed involvement in adhesion and osteogenic differentiation, confirming the ECM composition as key modulator of MSC behavior. In addition to known ECM components, proteomic analysis revealed novel ECM functions, which could improve culture conditions. In summary, this study provides a simplified method to obtain an *in vitro* MSC-derived ECM that enhances osteogenic differentiation and could be applied as natural biomaterial to accelerate bone regeneration.

Keywords: mesenchymal stromal cells, extracellular matrix, bone, bone tissue engineering

Introduction

Mesenchymal stromal cells (MSCs) are promising candidates for bone regeneration, because they can differentiate toward osteoblasts and secrete trophic factors that modulate target cells.[1,2] MSCs are combined with biomaterials for bone tissue engineering applications, and have been proposed to reduce skeletal defects.[3]

To accelerate bone regeneration, differentiation of MSCs into bone-forming cells is critical. *In vivo*, MSC-derived osteoblasts deposit the surrounding extracellular matrix (ECM) that is subsequently mineralized.[4] The most abundant protein of the ECM is collagen type 1 (COL1A1). Together with hydroxyapatite crystals, the ECM physically supports bone cells to regulate mineral deposition.

Furthermore, the bone ECM is a very dynamic tissue that contains and actively regulates the availability of growth factors (GFs) and signaling factors, such as bone morphogenic proteins (BMPs), and influences the signal transduction of these molecules. As a result, the ECM modulates MSC behavior, such as cell adhesion, proliferation, and commitment.[5,6] The specific composition of bone ECM is essential in this role. This is because proteoglycans and enzymes such as alkaline phosphatase (ALP) and matrix metalloproteinases (MMPs) enrich the ECM composition, along with the noncollagenous proteins (NCPs), such as osteonectin (SPARC), osteocalcin (BGLAP), osteopontin, and matrix gla proteins, which regulate collagen–fiber mineralization and cell–matrix adhesion.[5]

Recently, the ECM has become increasingly important as a natural 3D framework, which modulates cell behavior and mimics the *in vivo* tissue architecture.[7,8] Strategies combining ECM-coated scaffolds and MSCs have been proposed to improve the supportive role of scaffolds in bone

[1]Department of Internal Medicine, Erasmus University Medical Center, Rotterdam, The Netherlands.
Departments of [2]Precision and Microsystems Engineering and [3]Biomechanical Engineering, Delft University of Technology (TU Delft), Delft, The Netherlands.
[4]Proteomics Center, Erasmus University Medical Center, Rotterdam, The Netherlands.

regeneration.[9] In this context, *in vitro* cell-secreted ECMs have been produced according to several decellularization methods, and represent a suitable alternative to decellularized matrices from tissues.[10]

Cell-derived ECMs have been proposed for extensive *ex vivo* expansion of MSCs, as they promote proliferation and maintain the multilineage differentiation potential of MSCs.[11–13] Interestingly, osteoblast-derived ECM enhances the osteogenesis of MSCs.[14,15] Although known ECM components such as collagen, fibronectin (FN), laminin, perlecan, biglycan, and decorin were detected in these MSC-derived ECMs, their full composition is still under investigation.[12,16–19] Nevertheless, the specific protein composition of ECM mediates these effects through cell–matrix interactions; for instance, COL1A1 and vitronectin (VTN) promote osteogenesis, and FN influences MSC behavior.[6,20–22] However, key ECM bioactive regulators of MSC functions have not yet been identified. The full composition of the ECM is difficult to disentangle due to its complex structure.

The aim of this study was to generate a devitalized ECM from human osteoblast-differentiated MSCs and investigate its effect on the osteogenic differentiation of MSCs and bone formation *in vivo*. The protein composition of the ECM was investigated by mass spectrometry (MS) and compared with the human bone proteome,[23] to gain insight into how the ECM modulates MSC behavior and whether it mimics the *in vivo* bone microenvironment.

Materials and Methods

Culture and devitalization of MSCs

Human bone marrow-derived MSCs were obtained commercially (PT-2501; Lonza, Walkersville, MD). MSCs from a single donor at passage 7 were cultured in 12-well plates (5128 cells/cm^2; Greiner bio-one, Frickenhausen, Germany) in alpha-Mem (10% fetal bovine serum (FBS), pH 7.5, phenol-red free, Gibco BRL, Life technologies). After 2 days of culture in non-differentiating conditions, MSCs were cultured in osteogenic conditions for 11 days (medium was supplemented with 100 nM dexamethasone and 10 mM β glycerophosphate; Sigma-Aldrich, St. Louis, MO) to induce the osteogenic differentiation.

Before the onset of mineralization, MSCs were devitalized as represented in Figure 1A. In brief, MSCs were washed twice with phosphate-buffered saline (PBS; Gibco BRL, Carlsbad, CA), frozen at −80°C, and then thawed at room temperature, without PBS, for 20 min each. These steps were repeated three times and followed by a DNase I treatment for 30 min at 37°C (10 U/mL; Sigma-Aldrich). The devitalized matrix was gently rinsed three times with PBS, air dried in the culture hood, and stored at −20°C for at least 7 days before further experiments.

ECM characterization

The devitalized ECM was cultured in osteogenic medium for 6, 24, and 48 h and the metabolic activity of the devitalized ECM was assessed by a viability indicator (Presto Blue® Cell Viability Agent; Life Technologies) following manufacturer's instructions. Fluorescence was measured by a microplate reader (Victor X4™ Multimode Plate Reader, Perkin Elmer; excitation 530 nm, emission 590 nm). Live MSCs cultured in osteogenic conditions were used as positive control.

The absence of cells after the devitalization treatment was demonstrated by 4,6-diamidino-2-phenylindole (DAPI) nuclear staining (Sigma-Aldrich). MSCs cultured on plastic and on ECM for 24 h were used as positive control.

To measure the roughness, the matrix was produced on glass coverslips coated with poly-L-lysine (PLL) (Sigma-Aldrich), following the devitalization procedure. In brief, sterile glass coverslips had been coated with PLL for 10 min and washed three times with milliQ water before cell seeding. For the background measurements, the same treatment was applied to a coated coverslip without cells. A dynamic mode atomic force microscopy (AFM; NaniteAFM, Nanosurf GmbH, Germany) was used to measure the roughness of the ECM. Areas of 50×50 μm, 20×20 μm, and 5×5 μm were scanned in two different areas of the matrix surface with noncontact long cantilever reflex coating (NCLR) probes (Nanoworld AG, Switzerland). Images of 20×20 μm scanned areas were analyzed using Gwyddion.*

We quantified the roughness by drawing eight lines across each image and considering the amplitude of Roughness average (Ra) for each line, which is defined as the average deviation of all points of roughness profile from a mean line over the evaluation length. The Ra values of all the lines were eventually averaged to the final values. Measurements were representative of two independent experiments.

The surface of the devitalized ECM was imaged by scanning electron microscopy (SEM) using a JEOL JSM-IT100LA equipment (JEOL Europe BV, Nieuw-Vennep, The Netherlands). Samples were prepared as previously described.[24] In brief, devitalized ECM on PLL-coated coverslip was washed with PBS, fixed (4% paraformaldehyde, 1% glutaraldehyde in PBS, pH 7.4), rinsed in demineralized water, dehydrated sequentially in graded alcohols (50% for 15 min, 70% for 20 min, 96% for 20 min), air dried, and gold coated. Different areas of two replicates were examined at various magnifications.

Cell adhesion analysis

To observe the cell morphology and analyze the cell adhesion to the ECM by immunohistochemistry, the devitalized ECM was produced on polystyrene plastic. Next, MSCs in osteogenic conditions were cultured for 2, 4, and 8 h. Actin cytoskeleton was stained by rhodamine-conjugated phalloidin (Thermo Fisher Scientific); focal adhesions were observed by staining vinculin (Vinculin Abfinity™ recombinant rabbit monoclonal antibody, Clone 42H89 L44, Life Technology; as secondary antibody: FITC goat antirabbit IgG, BD Pharmigen) and observed by a fluorescent microscope (Zeiss Axiovert 200 MOT microscope). Images with a magnification of 630× were considered and processed with Image J (www.imagej.nih.gov/ij, version 1.47n), as previously described.[25]

In brief, the background was subtracted by using the Sliding Paraboloid option, the local contrast was enhanced by running the Clahe option, the Mathematical Subtract Function with a value of 10,000 was applied to subtract the background, followed by Mathematical Exponential (EXP) to further minimize the background. The contrast was adjusted using Brightness & Contrast tool. The number of

*www.gwyddion.net

focal adhesions relative to the area stained by phalloidin was quantified by Cell Profiler (www.cellprofiler.com, version 2.1.1). For the analysis, an average of four pictures with a magnification of 400× was considered, following the same steps as previously described with Image J, and analyzed using a self-made pipeline in Cell Profiler.

The morphology of cells cultured on the devitalized ECM and in standard culture conditions on PLL-coated coverslips was observed by SEM. Cells were cultured in osteogenic conditions for 24 h and processed as previously described[24] for the devitalized ECM. Images were acquired at various magnifications using secondary and backscattered imaging modes.

Cell adhesion was quantified by Flow Cytometry (Accuri C6 Flow Cytometer; BD Biosciences, San Jose, CA), using counting beads (Liquid Counting Beads; BD Biosciences). MSCs in osteogenic conditions were cultured for 6 and 24 h on ECM and plastic; after washing and trypsinization, the number of cells relative to a known concentration of fluorescent counting beads was counted. The result is representative of three independent experiments.

The heterogeneous MSC population was sorted based on ALP expression by fluorescence-activated cell sorting (FACS) (FACS Jazz; BD Bioscience) (ALP antibody: PE mouse antihuman ALP, clone B4-78; BD Biosciences). ALP-positive and ALP-negative sorted cells were seeded on the devitalized ECM in osteogenic medium, and cell adhesion was measured after 24 h of culture as previously described. Unsorted MSCs were used as control. Measurements were representative of two independent FACS experiments.

Cell proliferation analysis

For the measurement of proliferation, MSCs were cultured in osteogenic conditions on ECM and plastic dishes for 1, 3, and 5 days, and the percentage of Ki-67 positive cells was detected (Alexa Fluor 488 mouse antihuman Ki-67; BD Pharmigen) by Flow Cytometry (Accuri C6 Flow Cytometer; BD Biosciences), within the propidium iodide-positive population (PI solution; BD Biosciences). The result is representative of three independent experiments.

Culture of MSCs on ECM and analysis of osteogenic differentiation

ALP activity and ECM mineralization were measured in cell extracts of MSCs cultured in osteogenic conditions on ECM and plastic dishes for 19 days as previously described.[26] Mineralization was further confirmed by Alizarin red staining (ARS).[26] The result is representative of three independent experiments.

In vivo *ectopic bone formation analysis*

To check whether the ECM would promote *in vivo* ectopic bone formation by MSCs, MSCs on hydroxyapatite and tricalcium phosphate beta (HA-TCP) with and without ECM have been subcutaneously implanted in immunocompromised mice (nonobese diabetic/Scid IL2R gamma (NSG), Charles River Laboratories). ECM was produced and devitalized on 20 mg of HA-TCP (Triosite™; Zimmer Biomet, Warsaw, IN) powder, following the same devitalization procedure as previously described.

HA-TCPs were loaded with MSCs (0.5×10^6/HA-TCP-pellet) in growth medium, let them attach overnight and subcutaneously implanted into four dorsal pockets in NSG mice ($N = 3$) (10 weeks old, females and males) under anesthesia, as previously described.[27] ECM on HA-TCP and HA-TCP vehicle were used as controls. A schematic overview is presented in Figure 4A. Three independent experiments with similar sample size were performed. All animal procedures were approved by the Committee on the Ethics of Animal Experiments of Erasmus University Medical Center, Rotterdam, The Netherlands. Mice were kept in pathogen-free facility, with 12 h/12 h light/dark cycle, controlled temperature (22°C ± 1°C) and humidity (50% ± 5%), and fed *ad libitum* with standard rodent diet.

All pellets were retrieved 8 weeks after implantation and ectopic calcification was checked by Masson–Goldner staining. In brief, pellets were fixed in 70% ethanol, dehydrated in graded alcohols, plastic embedded (methyl methacrylate, MMA), and cut into 6-μm-thick sections by microtome (RM2255; Leica Biosystem). Two stained sections of each pellet (one from the periphery of the pellet and one from the core) were scanned by Nanozoomer 2.0 HT (Hamamatsu Photonics), and areas of newly formed mineralized bone over HA-TCP were quantified by Image J (www.imagej.nih.gov/ij, version 1.47n), by two independent observers blind toward the data (as represented in Supplementary Fig. S1A–C. Supplementary Data are available online at www.liebertpub.com/tea).

MS analysis

The proteomic composition of ECM was analyzed by MS, with a label-free quantification (LFQ) method. ECM samples were scraped and collected in 0.5 mL of PBS Triton 0.1% and concentrated by using centrifugal filters (Amicon Ultra-0.5 mL centrifugal filters, Millipore; 3KDa cutoff) following manufacturer's instructions. Protein content was quantified by BCA kit (Pierce Biotechnology, Rockford, IL) following manufacturer's instruction. Protein extracts (2.5 μg) were reduced by NuPAGE® reducing agent and resolved by one-dimensional SDS-Page gel, in duplicate (NuPAGE®Novex® 4–12% Bis-Tris-Acetate Gels; Life technologies). Protein bands were stained with Coomassie staining (Bio-safe Coomassie; Bio-Rad, Hercules, CA) for 1 h and destained in milliQ water overnight. Samples were processed as previously described.[28]

In brief, an automatic gel slicer was used to cut gel lanes into 2-mm slices, which were subsequently in-gel reduced with dithiothreitol, alkylated with iodoacetamide, and digested with trypsin (Promega, sequencing grade, Madison, WI). A 1100 series capillary LC system (Agilent Technologies) coupled to an LTQ-Orbitrap XL mass spectrometer (Thermo Scientific) was used in positive mode to perform Nanoflow LC-MS/MS. ReproSil C18 reversed phase column (Dr. Maisch GmbH; 1.5 cm × 100 μm, packed in-house) was used to trap the peptide mixtures at a flow rate of 8 μL/min.

Peptides were separated by a linear gradient from 0% to 80% B (A = 0.1% formic acid; B = 80% (v/v) acetonitrile, 0.1% formic acid) in 170 min, at a constant flow rate of 200 nL/min, using a splitter, on ReproSil C18 reversed phase column (Dr. Maisch GmbH; Ammerbuch-Entringen, GE; 15 cm × 50 μm, packed in-house). The eluent was directly sprayed from the column into the ESI source of the mass spectrometer. Peptides were fragmented in data-dependent mode, and mass spectra were acquired in continuum mode. The MS proteomics data have been deposited to the

ProteomeXchange Consortium through the PRIDE[29] partner repository with the data set identifier PXD006865 (Username: reviewer20352@ebi.ac.uk; Password: LC3okFPV).

Bioinformatic analysis

The MaxQuant Software (version 1.5.0.0) was used to analyze the raw MS data, with a false discovery rate of 0.01 for proteins and peptides and six amino acids as minimum peptide length. The MS/MS spectra were searched by Andromeda search engine, against the human proteome as provided by Uniprot database (taxonomy: *Homo sapiens*, release HUMAN_2013_04) (uniprot.org, v2014_05), with the reversed versions of all the sequences (maximum of two missed cleavages; 0.6 Da fragment mass tolerance, enzyme specificity: trypsin). Samples were run in duplicates and then averaged for the analysis. LFQ values >0 were considered for the analysis. Over-represented gene ontology (GO) terms were analyzed by using DAVID Bioinformatic Resources v6.7,[30] using the whole human genome as background. Only significantly enriched terms (Benjamini $p < 0.01$) were considered.

The protein composition of the devitalized ECM was compared with one of three human bone samples that we previously described.[23] The shared proteins between the two data sets were analyzed through QIAGEN's Ingenuity® Pathway Analysis (IPA®, QIAGEN Redwood City www.qiagen.com/ingenuity).

Immunoblot analysis

The presence of some proteins detected by MS in the ECM was confirmed by Western blot. In brief, ECM samples (12 μg) were prepared as for MS analysis, mixed with 6× reducing sample buffer, separated by SDS-PAGE, and transferred onto nitrocellulose membrane (Hybond-ECL; Amersham Bioscience, Buckinghamshire, United Kingdom). After nonspecific blocking with 5% BSA in Tris-buffered saline 0.1% Tween-20, membranes were incubated overnight with primary antibody against FN1 (mouse monoclonal to FN1, 1:5000, Ab-11, Clone FBN11; Termo Fisher Scientific, Rockford, IL), ALP (mouse monoclonal to ALP, 1:1000, Clone 0.G.2; Abcam, Cambridge, United Kingdom), ANXA2 (rabbit polyclonal, 1:1000; Abcam), and GAPDH loading control (mouse monoclonal, 1:1000, Clone sc-69778; Santa Cruz Biotechnology, Dallas, TX).

Membranes were probed with secondary antibody conjugated with goat antimouse Alexa Fluor 680 (goat antimouse, 1:300; Invitrogen, Waltham, MA) and IRDye 800CW (goat antirabbit, 1:5000; LI-COR, Lincoln, NE). Bands were observed using the LI-COR Infrared Imaging System (LI-COR) according to manufacturer's instruction.

Statistical analysis

Data are representative of multiple independent experiments. All values are presented as average ± standard deviation (SD) of biological replicates, and significance was calculated by two-way analysis of variance, followed by Bonferroni *Post Hoc* test, otherwise indicated elsewhere.

Results

Preparation of MSC-derived ECM

To study the impact of the ECM on MSC behavior, we successfully produced an *in vitro* model of devitalized ECM by using freeze/thaw cycling as decellularization technique. As schematically represented in Figure 1A, MSCs were osteogenically differentiated to allow the production of the ECM, and before the onset of mineralization, devitalized by freeze/thaw cycles, followed by a DNAse treatment. Extensive washings were intended to withdraw the potential remaining live cells and the cellular debris. Taking advantage of an adaptation of a previous protocol,[31] this devitalization procedure represented a simplified way of producing an *in vitro* cell-secreted ECM.

The ECM was metabolic inactive after the devitalization treatment and exhibited a rough surface

As the devitalization treatment should remove cells to minimize immune response, while maintaining the bioactivity of the matrix,[9] we checked the efficacy of the devitalization treatment by using Presto Blue. Figure 1B illustrates that the devitalization treatment completely abolished the viability of the cells. In fact, although the metabolic activity of live MSCs increased over time as expected, the matrix remained metabolically inactive. DAPI nuclear staining showed that cells were absent after devitalization treatment (Supplementary Fig. S1D). This confirmed the validity of the devitalization treatment used to prepare the MSC-derived ECM.

Next, we analyzed the surface of the devitalized ECM by AFM. AFM images of the scanned areas showed that the matrix had a rough surface, and exhibited fiber-like structures relative to the featureless PLL-coated surfaces (Fig. 1C). Quantified data revealed a roughness of 12.75 nm for the ECM compared with 4.53 nm for the PLL-coated surface without cells, as shown in Figures 1C, D. Investigations of larger areas of devitalized ECM by SEM confirmed the rough surface and the presence of fibrous structures and aggregates (Fig. 1E).

The ECM increased MSC adhesion

Next, we investigated whether the devitalized ECM could enhance cellular attachment. Therefore, we analyzed the effect of the devitalized ECM on the adhesion of freshly seeded human MSCs.

Figure 2A illustrates that MSCs adhere more efficiently and quicker on the devitalized ECM than on plastic. Within 2 h after seeding the cells, the actin cytoskeleton was correctly organized to shape a proper morphology, as shown by phalloidin staining, whereas this was not yet the case for the MSCs seeded on plastic. In addition, vinculin staining showed that MSCs on ECM formed focal adhesions within 2 h after seeding. At this time point, the number of focal adhesions per area stained by phalloidin in cells on ECM was >18-fold higher than in cells seeded on plastic. Although not significant, the number of focal adhesions was overall higher at each time point (Supplementary Fig. S1E). These analyses illustrate that seeding cells on a preformed ECM significantly accelerates MSC adhesion.

MSCs cultured for 24 h on the devitalized ECM and in standard culture conditions exhibited a stretched morphology with focal adhesion complexes, but no substantial differences in morphology were highlighted when imaged at high magnification by SEM (Fig. 2B). However, an increased number

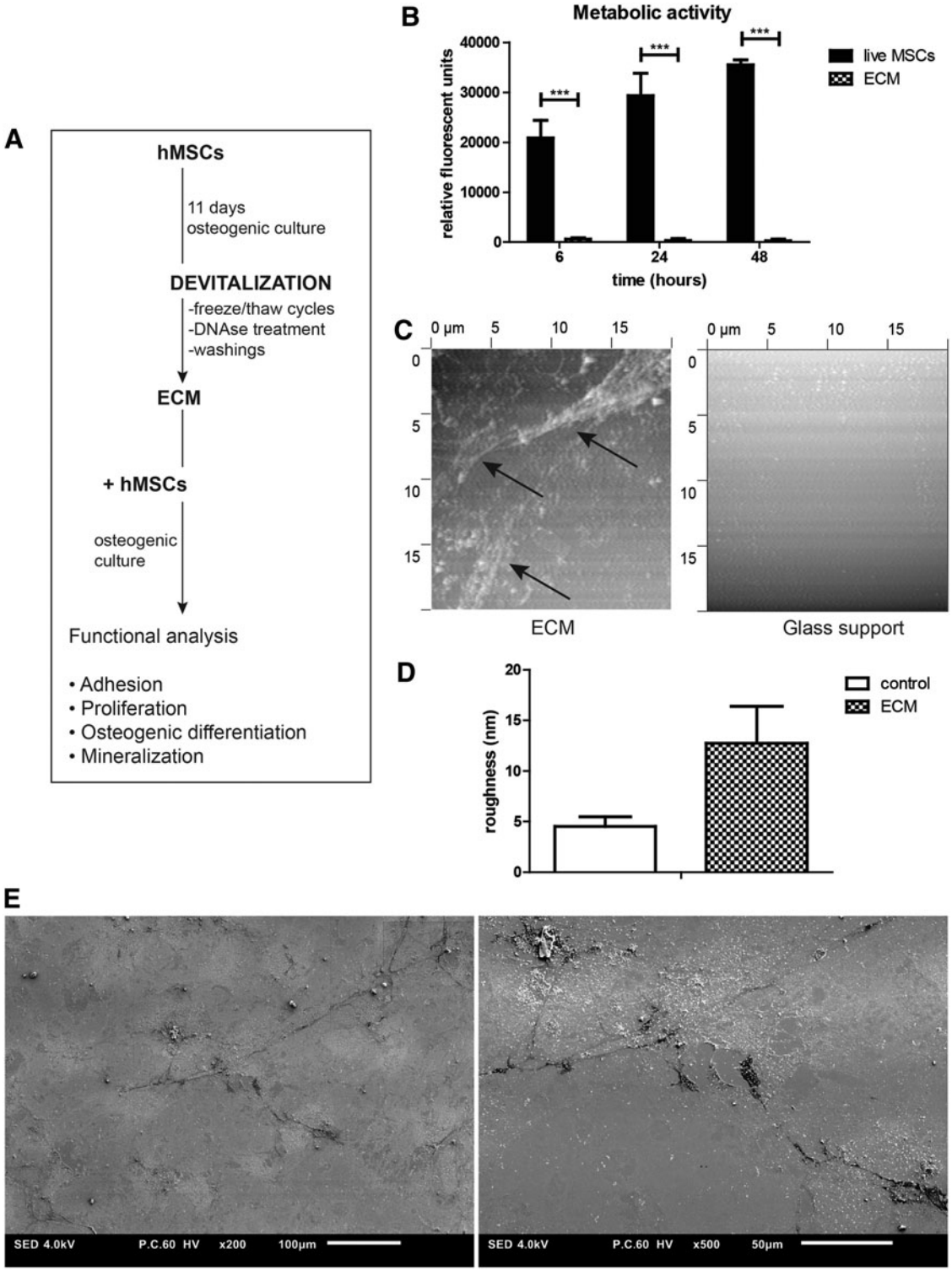

FIG. 1. Preparation and characterization of MSC-derived ECM. **(A)** Schematic overview of ECM preparation and culture conditions. **(B)** Metabolic activity of ECM and live MSCs measured at 6, 24, and 48 h after seeding with Presto Blue viability agent. Values are presented as relative to blank (osteogenic medium with Presto Blue) (***$p < 0.001$) ($N = 3$). **(C)** AFM images of ECM and control (20×20 µm scans) on a glass substrate. Images represent the topography of the area analyzed, coming from the oscillation of the cantilever over the scanned surface. *Black arrows* indicate fiber-like structures. **(D)** Roughness quantification of ECM and control, based on amplitude of average roughness (Ra) values from independent scans. Values: average ± SD. **(E)** Scanning electron micrographs of the surface of devitalized ECM at 200× (*left*) and 500× magnification (*right*). Images are representative for multiple areas in two specimens. Scale bars indicate 100 µm (*left*) and 50 µm (*right*). AFM, atomic force microscopy; ECM, extracellular matrix; MSC, mesenchymal stromal cell.

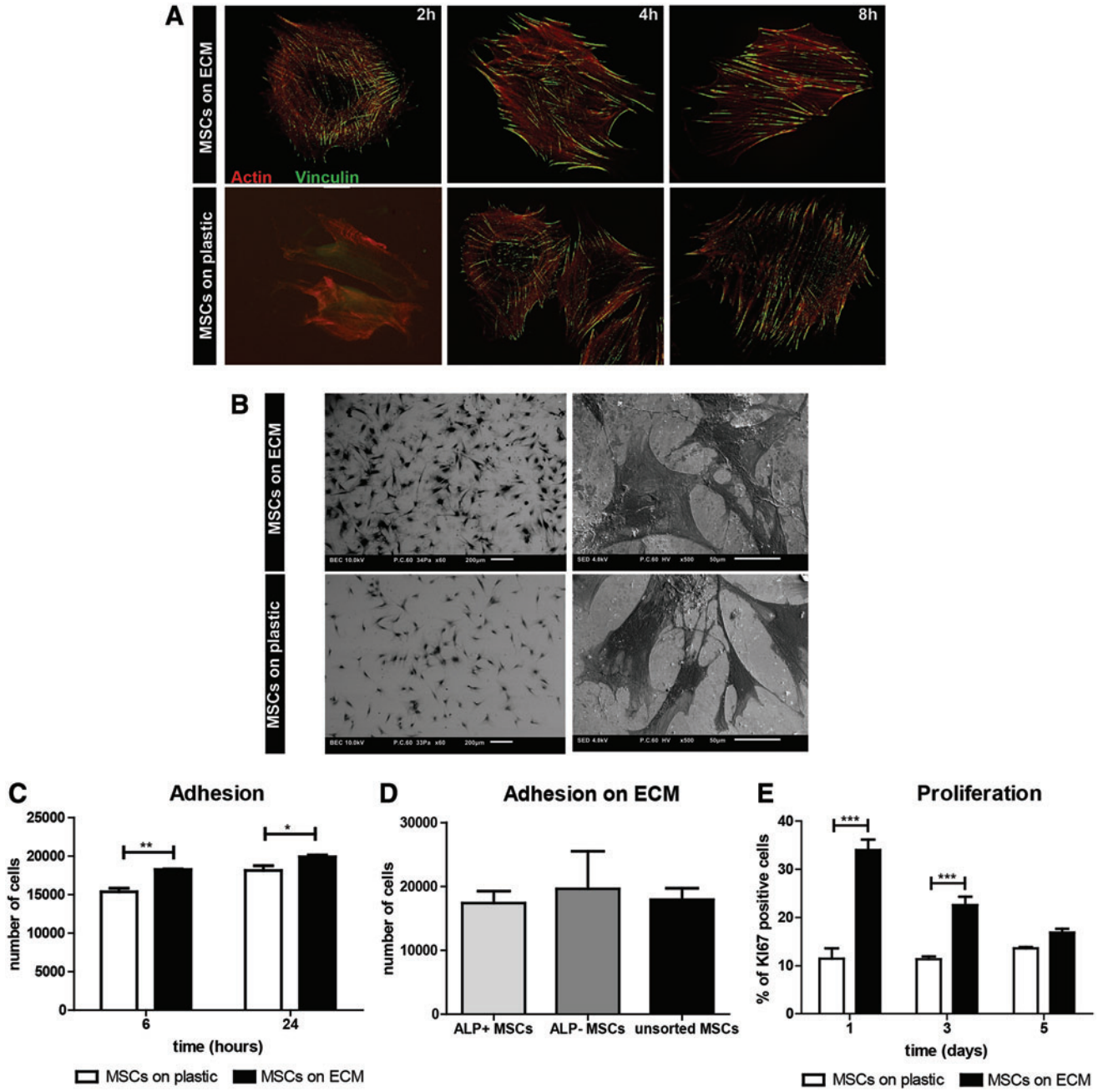

FIG. 2. ECM enhances MSC adhesion and proliferation. **(A)** Immunohistochemistry of MSCs on ECM (*top*) and plastic (*bottom*) at 2, 4, and 8 h after seeding. *Red*, phalloidin for actin cytoskeleton; *green*, vinculin of focal adhesions. **(B)** SEM images of MSCs cultured on the devitalized ECM (*top*) and in standard culture conditions (*bottom*) for 24 h, at 60× (*left*) and 500× magnification (*right*). Images are representative of multiple areas in two specimens. Scale bars indicate 200 μm (*left*) and 50 μm (*right*). **(C)** Quantification of cells in adhesion to substrates counted by flow cytometry. **(D)** Quantification of MSC subsets (ALP positive-, ALP negative-sorted cells, and unsorted cells) in adhesion to the ECM for 24 h, counted by flow cytometry (no significant difference was detected by one-way analysis of variance, followed by Bonferroni's multiple comparison test). **(E)** Proliferation of MSCs on ECM and on plastic as percentage of Ki-67-positive cells by flow cytometry. Results are representative of multiple independent experiments. (*$p < 0.05$; **$p < 0.01$; ***$p < 0.001$). Values: Average ± SD. ALP, alkaline phosphatase. Color images available online at www.liebertpub.com/tea

of cells were generally observed on the devitalized ECM relative to the standard culture conditions.

The increased cell adhesion was further confirmed by counting the number of cells that adhere to the different substrates. Six hours after seeding on the ECM, the number of cells was 1.2-fold ($p < 0.01$) higher than on plastic, and 1.3-fold ($p < 0.05$) higher after 24 h (Fig. 2C).

In addition, we investigated the preferential adhesion of MSC subsets to the devitalized ECM. We focused on ALP-positive MSCs, considered as already osteogenic committed

MSCs, and ALP-negative MSCs, considered as yet uncommitted MSCs. Hereto we fluorescence-activated cell sorted the heterogeneous population of MSCs based on ALP expression, and next seeded the ALP-positive and ALP-negative population on the devitalized ECM. After 24 h of culture, no significant difference was detected in the adhesion of these subsets and the unsorted population (Fig. 2D). The devitalized ECM was able to bind not only the committed ALP-positive MSCs but also the ALP-negative cells.

The ECM increased MSC proliferation and accelerated MSC osteogenic differentiation and mineralization in vitro

We investigated whether the accelerated attachment to the devitalized ECM was accompanied by an effect on cell proliferation, by analyzing the percentage of Ki-67-positive cells by flow cytometry. After 1 day of culture of MSCs on ECM, 34% of the cells were Ki-67 positive, whereas only 11% of the cells were positive when cultured on plastic. This illustrates that 24 h of culture on ECM was sufficient to increase the number of proliferating MSCs by 2.97-fold (Fig. 2E). The percentage of Ki-67-positive cells gradually decreased in time to similar levels as the cells seeded on plastic. After 5 days of osteogenic differentiation, the percentage of proliferating cells lowered to 16%.

Next, the influence of the ECM on the osteogenic differentiation of MSCs was studied. MSCs cultured on ECM differentiated faster toward osteoblasts than those grown on plastic. After 11 days of differentiation, ALP activity in MSCs cultured on ECM was 2.2-fold higher than their counterpart on plastic (Fig. 3A). Furthermore, mineralization was accelerated and increased by culturing MSCs on the ECM, as illustrated by calcium deposition in the well and the ARS (Fig. 3B–D). The amount of calcium deposited after 19 days of culture, as measure of mineralization, was >20-fold higher in MSCs cultured on ECM than on plastic (Fig. 3B). ARS of the mineralized ECM confirmed the increased mineralization of cells seeded on devitalized ECM, as shown in Figure 3C, D.

ECM promoted in vivo *ectopic bone formation by MSCs*

Based on the osteopromotive role of the ECM on MSCs *in vitro*, we investigated whether the ECM influenced the *in vivo* bone formation by MSCs in an ectopic calcification model.

MSCs with and without ECM were subcutaneously implanted on HA-TCP in immunocompromised mice and bone

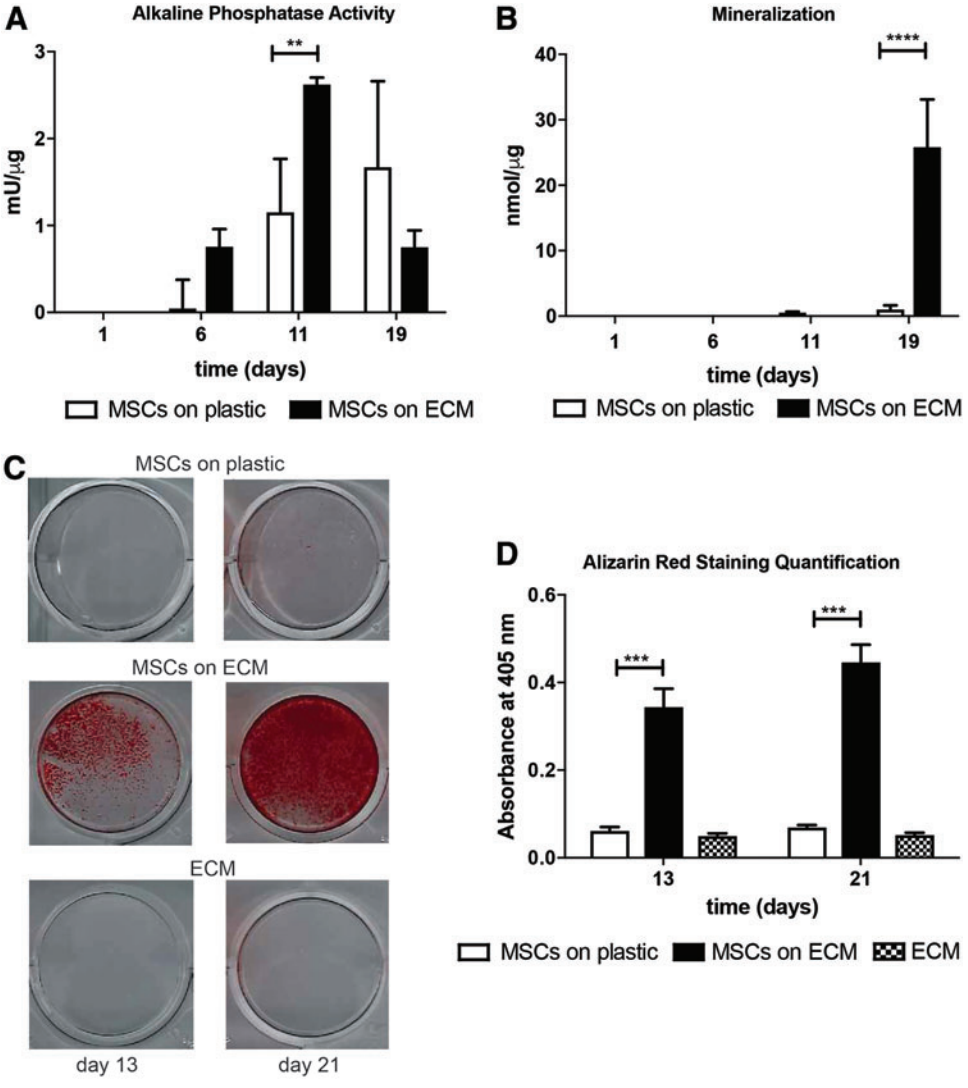

FIG. 3. ECM accelerates MSC osteogenic differentiation and mineralization. **(A)** ALP activity in cell extracts of MSCs on ECM and plastic. **(B)** Calcium deposition in cell extracts of MSCs cultured on ECM and plastic. The values of MSCs on ECM were subtracted by the ECM contribution. All values are corrected for protein content at each time point. Negative values were artificially set as 0. The provided results are representative of multiple independent experiments. **(C)** Alizarin Red Staining (ARS) at days 13 and 21 of culture, in MSCs on plastic (*top*), MSCs on ECM (*middle*), and ECM only (*bottom*). **(D)** Quantification of ARS at days 13 and 21 of culture. (**$p < 0.01$; ***$p < 0.001$, ****$p < 0.0001$). Values: Average ± SD. Color images available online at www.liebertpub.com/tea

formation checked by Masson–Goldner staining after 8 weeks, as represented in Figure 4A. Histological evaluation showed that MSCs on HA in this experimental setup induced ectopic bone formation (Fig. 4B, C). In two out of three experiments, MSCs implanted with ECM gave rise to about 20-fold higher amount of bone than when ECM was not present (Fig. 4D). In the experiment that did not show an effect of ECM, the bone formation in control HA-TCP was already at the level induced by the ECM conditions in the other experiments, potentially explaining that an additional increase was not observed.

Overall, in contrast to the control condition, the presence of ECM robustly led to ectopic bone formation in all experiments (Fig. 4D). Ectopic bone formation was not detected when HA-TCP pellets were loaded without MSCs (Supplementary Fig. S1F).

The proteomic composition of the ECM corroborated the role of the devitalized matrix in mediating the observed effects on MSCs

Following these positive effects of the devitalized ECM on cell adhesion, proliferation, and osteogenic differentiation of MSCs, we investigated the protein composition of the ECM, to identify candidate proteins and processes underlying these effects. MS analysis identified 846 proteins that were part of the devitalized ECM (Supplementary Table S1). Of these 846, 35 proteins were annotated as ''extracellular matrix'' GO term (GO:0031012) (Fig. 5A). The detection of known ECM components such as FN, COL1A1, and tenascin C (TNC) within the most abundant proteins in the devitalized ECM confirmed the presence of a bone-like ECM and the validity of the devitalization treatment to produce the ECM. The presence of proteins detected by MS in the devitalized ECM such as FN, Annexin2 (ANXA2), and ALP was confirmed by Western blot analysis (Fig. 5B).

As illustrated in Figure 5C, GO analysis revealed that the top 10% most abundant proteins (85 proteins) were involved in cell–matrix adhesion processes, as integrin binding (GO:0005178) was significantly enriched. Furthermore, GO terms such as membrane-bounded vesicle (GO:0031988) and calcium ion binding (GO:0005509), which included proteins such as ANXA2, ANXA5, and ANXA6, were also enriched in our analysis (Supplementary Table S2). As these proteins are involved in matrix vesicle release, calcium ion binding, and, therefore, mineralization, this suggested the role of the ECM in promoting the osteogenic differentiation and mineralization of MSCs. ALP was also detected and ranked in position 142 of abundance (Fig. 5A, B and Supplementary Table S1). However, ALP appeared to be inactive as the ECM lacked ALP activity (Supplementary Fig. S1G).

The GO analysis of the whole composition of the ECM shown in Figure 5D illustrates that the GO term ECM organization (GO:0030198) was significantly enriched, meaning that the total composition of ECM was important for the structure of the devitalized ECM, and not only the most abundant proteins. Furthermore, Figure 5D illustrates that GO terms such as antioxidant activity (GO:0016209), mitochondrion (GO:0005739), and vasculature development (GO:0001944) were significantly enriched (Supplementary Table S3).

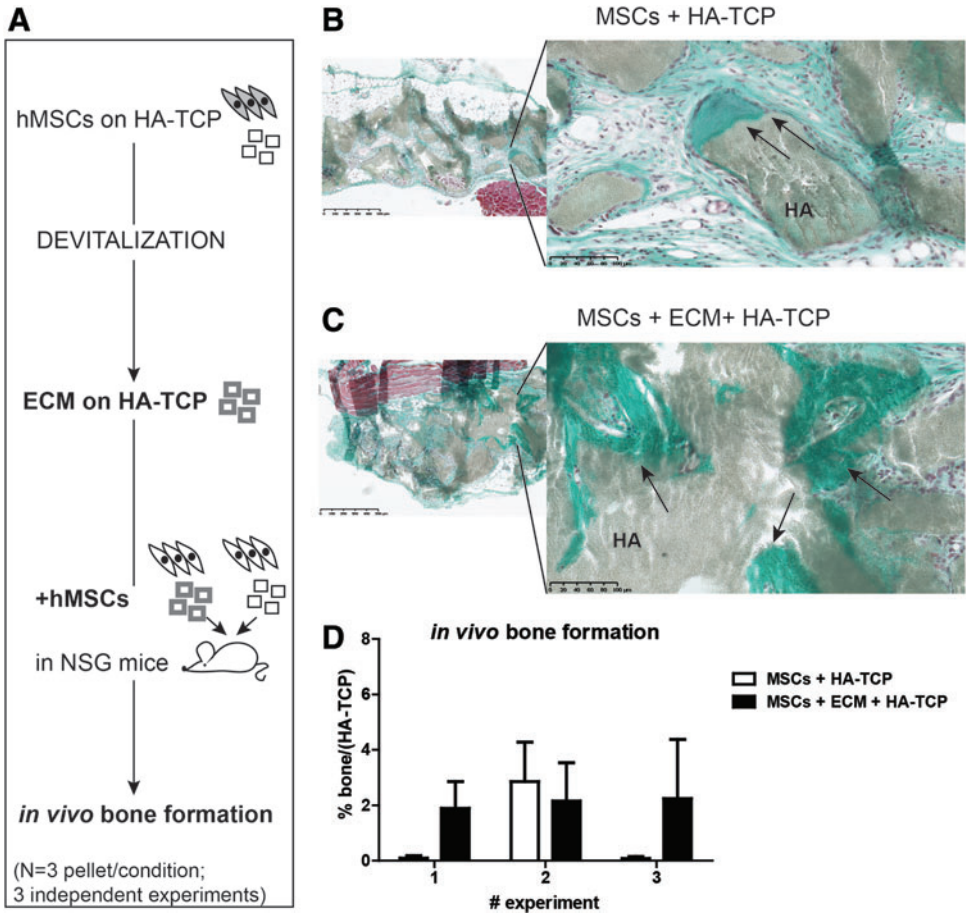

FIG. 4. MSCs on ECM on HA-TCP promote ectopic bone formation *in vivo*. **(A)** Schematic overview of *in vivo* implantation experiment. **(B)** Histological analysis of newly formed bone by MSCs on HA-TCP and **(C)** MSCs on ECM on HA-TCP. Two sections/pellet, four pellets/condition, in three independent experiments were analyzed and representative sections are shown. *Arrows* indicate the newly formed bone stained in *green* by Masson–Goldner staining on HA-TCP (indicated as HA). *Light pink* areas indicated unmineralized bone and *purple dots* indicate nuclei. Bars indicate 500 μm (*left*) and 100 μm (*right*). **(D)** Quantification of the newly formed bone by MSCs on ECM on HA-TCP and MSCs on HA-TCP in each experiment. Three independent experiments are shown. Values: Average ± SEM of percentage bone/(HA-TCP) in pellets per each experiment. HA-TCP, hydroxyapatite and tricalcium phosphate beta. Color images available online at www.liebertpub.com/tea

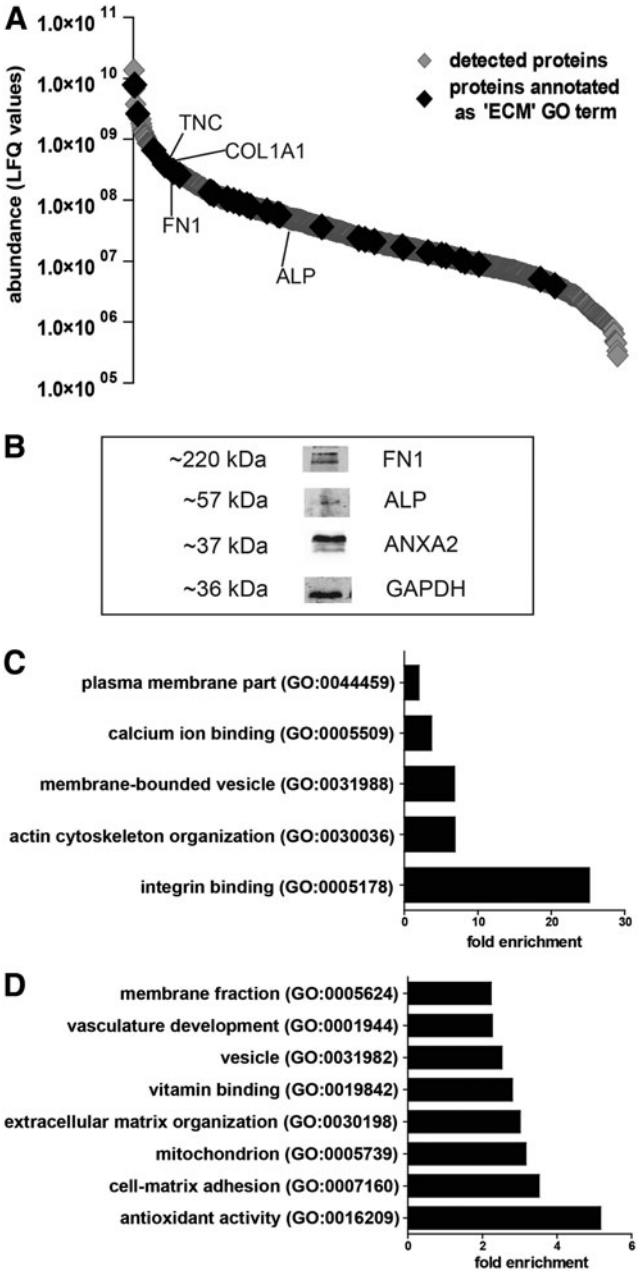

FIG. 5. Proteomic analysis of the ECM composition. **(A)** A total of 846 proteins were detected by mass spectrometry; 35 were annotated as ''extracellular matrix'' GO term. Some of the most relevant proteins are indicated. **(B)** Western blot analysis of FN1, ALP, and ANXA2 (12 μg loaded) in the devitalized ECM. GAPDH was used as loading control. **(C)** Gene ontology (GO) analysis of the top 10% most abundant detected proteins. **(D)** Most enriched pathways of GO analysis of all the proteins detected in the ECM. Only the significantly enriched terms are shown (Benjamini $p < 0.01$).

The devitalized ECM showed high protein homology with human bone samples

We have previously analyzed the composition of the human bone proteome,[23] showing 1213 proteins that were shared by three human bone samples. Further analyses lowered them down to 1200 unique proteins. This human bone proteome was compared with the protein composition of the *in vitro* cell-secreted ECM. More than 50% of the ECM proteins were shared with the bone proteome, as 473 proteins out of 846 detected in the devitalized ECM were also detected within the human bone samples (Fig. 6A). Annexins such as ANXA2, ANXA6, ANXA5, ANXA1, and vimentin (VIM) were within the most abundant proteins in the ECM that were also detected in the bone proteome (Supplementary Table S4).

Bioinformatic analysis of the shared proteins showed that specific osteoblast- and ECM-related terms such as ''adhesion of cell-associated ECM,'' ''differentiation of osteoblasts,'' and ''proliferation of connective tissue cells,'' were significantly enriched (Fig. 6B), confirming the role of the protein composition of the ECM in mediating these effects. Proteins such as trombospondin-1 (THBS1), VTN, and FN, but also intracellular proteins such as integrins, were within the 473 shared proteins, and were involved in ''adhesion of cell-associated matrix.'' Moreover, proteins such as SPARC, COL1A1, and fibulin-1 (FBLN1) were related to the proliferation of connective tissue cells, whereas TNC, VIM, and Versican were responsible for the differentiation of osteoblasts, overall confirming the role of the ECM in mediating the functional effects we observed (Supplementary Table S5).

Discussion

In this study, we successfully produced an osteopromotive human MSC-derived ECM, which was able to accelerate the adhesion, proliferation, and osteogenic potential of MSCs *in vitro* and to promote ectopic bone formation *in vivo*. Known ECM components were detected in the devitalized ECM, which also showed high homology with the human bone protein composition. This validated our ECM model and provided insights into how the ECM may modulate MSC behavior. Moreover, many unexpected proteins not directly related to ECM structural role were also detected.

Immediately after seeding on the ECM, MSCs formed focal adhesion complexes that improved their adhesion to the devitalized ECM. Extracellular proteins, such as FN, COL1A1, VTN, and TNC, favor osteoblast adhesion to the ECM by creating cell–matrix adhesion sites.[6,20] The proteomic analysis of the devitalized ECM identified FN, COL1A1, and TNC within the most abundant proteins, and other adhesive extracellular proteins, such as VTN and FBLN1. Together this confirmed the presence of cell adhesion promotors in the devitalized ECM, explaining the accelerated cell attachment. Moreover, the devitalized ECM was able to enhance the attachment of MSCs irrespectively of their commitment, as less committed cells attached on the ECM to a similar extent than the more committed cells.

One day on the devitalized ECM was already sufficient to increase the percentage of proliferating MSCs, confirming previous findings that used different cell-secreted ECMs to enhance MSC proliferation.[11–13,16] By analyzing the proteomic composition of the ECM, we could successfully detect FN, COL1A1, and SPARC, which have been shown to promote osteoblast proliferation,[22,32] and TNC, which may mediate transforming growth factor beta (TGF-β) action on bone formation.[33] The percentage of proliferating cells decreased over time as cells started to differentiate.

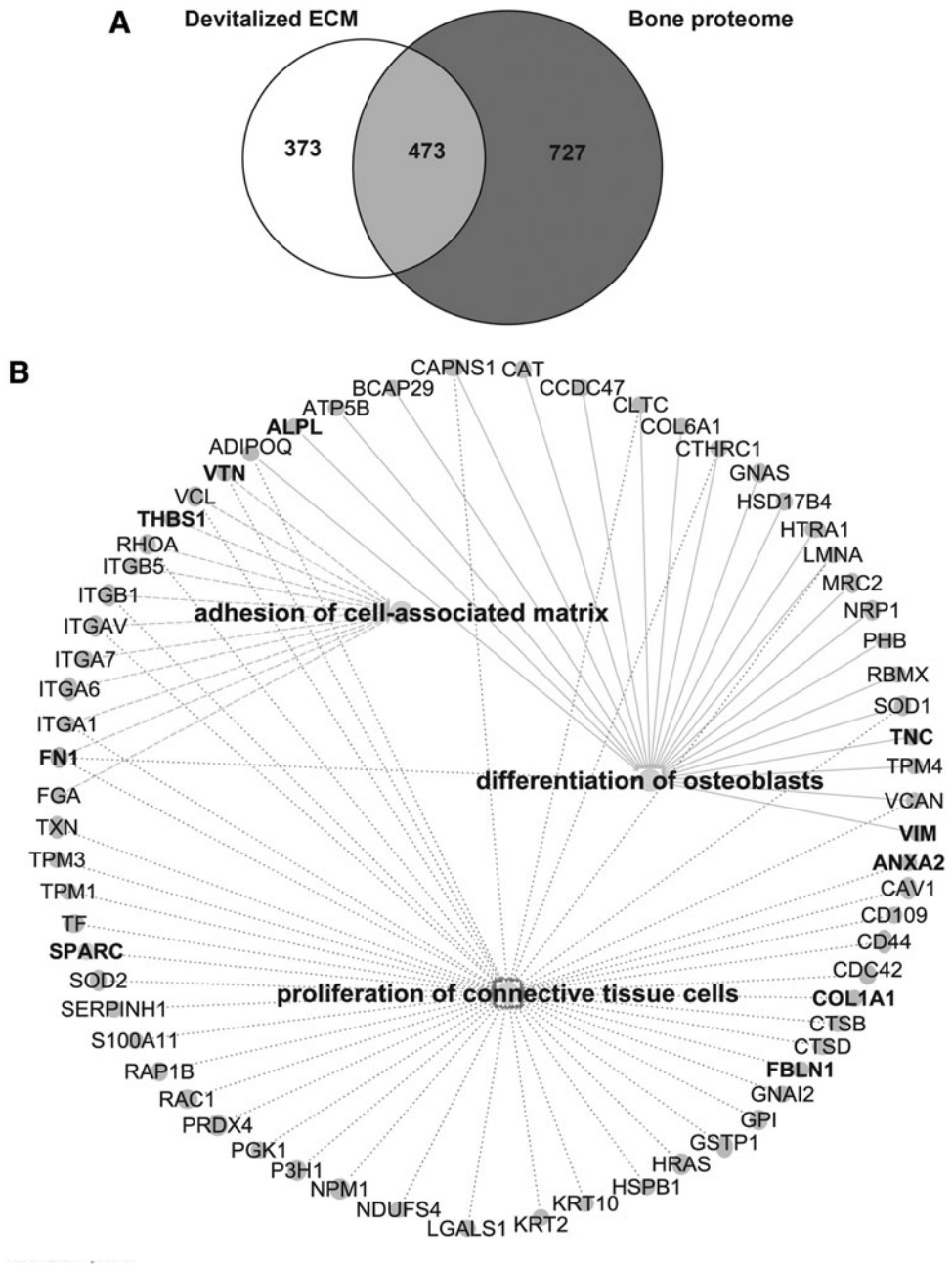

FIG. 6. Comparison of the protein composition of the devitalized ECM and the human bone proteome. **(A)** A total of 473 proteins were shared between the devitalized ECM and the human bone proteome. **(B)** Ingenuity pathway analysis of the 473 proteins shared between the devitalized ECM and the human bone samples. Represented proteins lead to the significant enrichment of functional annotations such as ''proliferation of connective tissue cells'' ($p = 3.81$ E-09), ''differentiation of osteoblasts'' ($p = 6.44$ E-07), and ''adhesion to cell-associated matrix'' ($p = 1.89$ E-06) (*bold*: proteins highlighted in the text).

The devitalized ECM induces a faster differentiation of MSCs toward mineralizing osteoblasts as both ALP activity and matrix mineralization were higher when MSCs were cultured on the ECM. This observation is supported by previous findings showing *in vitro* cell-secreted ECMs that promoted osteogenesis.[14,15] The quicker adhesion to the known osteogenic inducers that were detected in the ECM, such as COL1A1, FN, collagen type XII alpha 1 (COL12A1), TNC, VTN, and SPARC, might activate integrin-mediated signaling pathways, increasing osteogenic differentiation.[5,20,22,33,34] Annexins such as ANXA2, ANXA5, and ANXA6 were detected in the devitalized matrix, along with previous findings.[17] Annexins are the initiators of mineralization and were also detected within the most abundant proteins in human bone samples, confirming the role of the devitalized ECM in mimicking the osteogenic bone microenvironment.[23,35]

Despite the detection of initiators of mineralization such as Annexins and ALP, the ECM has low ALP activity and does not mineralize without further presence of living cells. The necessity of living cells may be conceptually important for the therapeutic application of devitalized ECM. If the ECM mineralizes independently of living cells, this would lead to uncontrolled mineralization, and may lead to pathological heterotopic mineralization. As osteoblast differentiation and bone formation are complex processes in which timing, order, and magnitude of events are important, inappropriate timing of mineralization thus may lead to an inappropriate bone repair process.

Bone formation induced by ECM directly implanted *in vivo* or by MSCs expanded on ECM *ex vivo* has shown conflicting findings.[10] We showed that the ECM promoted *in vivo* ectopic bone formation by MSCs, inducing a higher

amount of bone than by MSCs alone. Probably the role of ECM is decisive to stimulate a robust formation of bone. However, further experiments are needed to increase the sample size and diminish the heterogeneity to overcome the biological variation. Based on our current observations, we propose that with any given MSC preparation, one may or may not observe bone formation, whereas in the presence of the ECM we produced, bone formation will be observed with all MSC preparations. In other words, the presence of the ECM seemed to reduce variation in the amount of bone formed over different experiments.

Structural ECM proteins and known components of the bone marrow niche, such as COL1A1, FN, VTN, and TNC, were successfully detected among the most abundant proteins in the ECM, along with previous findings.[12,16–18]

However, also inhibitors of mineralization were detected, such as alpha-2-HS-glycoprotein, which is found in the mineralized bone but also acts as inhibitor of ectopic calcification.[36] Interestingly, GFs such as BMPs and TGF-β could not be detected in the ECM, which may be attributed to the sensitivity of the technique or to the devitalization procedure. Despite the absence of GFs, we unequivocally show that the matrix influenced MSC behavior. Probably, ECM remodeling takes place, releasing GFs that were entrapped in the ECM. Indeed, protease inhibitors such as cystatin C (CST3) were detected, but also proteinases, such as matrix metalloproteinase 14 (MMP14), which are known to promote osteogenic differentiation.[37,38]

Notably, many proteins detected in the devitalized matrix were annotated as cytoplasmic or plasma membrane bound. Cell remnants most likely arose from cell lysis during the freeze–thaw cycling and were resistant to the extensive washings.[10] Nevertheless, we should consider that the ECM composition in its entirety was responsible for the effects described in this study; these proteins enriched the matrix composition, playing a central role with the known ECM proteins.

As >50% proteins were shared between the devitalized ECM and the human bone samples, we thus show that our natural ECM model is representative of the *in vivo* dynamic bone microenvironment. Following this, cell remnants may have a functional role as remnants arising from osteoblasts undergoing apoptosis. These are present in the bone and bone marrow and stimulate efferocytosis by osteal macrophages, which are key regulators of bone homeostasis and wound repair.[39] Therefore, the cell remnants detected in the devitalized ECM could implement the supportive role of stromal cells and thereby the ECM we produced may represent a more complete environment than just the well-known ECM proteins. However, further studies are needed to unravel new functions for the ECM in the context of osteoimmunology.

We unexpectedly detected many proteins related to mitochondrial functions and structure in the devitalized matrix. Nevertheless, we show that the devitalized matrix is metabolically inactive. As the osteogenic differentiation is a high-energy demanding process, we believe that these proteins arise from lysis of the ECM-secreting MSCs, as the devitalization occurred before the onset of mineralization and might be related to energy metabolism function.

GO analysis of the proteins detected in the ECM revealed also GO terms that were not directly related to known ECM functions, thus broadening the spectrum of the devitalized ECM functions. For instance, ''antioxidant activity'' appeared as an enriched GO term, with proteins such as superoxide dismutase 1 that was previously detected in the human bone microenvironment.[23] As the ECM has been already proposed to reduce MSC aging,[13] the antioxidant function of the devitalized matrix should be further investigated to improve *ex vivo* cultures for clinical applications.

The most abundant proteins detected in the matrix were also related to angiogenesis and vasculature remodeling, showing interesting functions of the ECM. Indeed, among these proteins, TNC is mitogenic for hematopoietic stem cells (HSCs) in HSC niche,[40] and COL1A1 is involved in vasculature remodeling.[41] Our findings support the idea of using the matrix for HSC expansion.[16]

The role of ECM in modulating MSC behavior has been successfully investigated in many studies using cell-secreted ECMs, which have been obtained by different decellularization techniques. Although the freeze–thaw cycles approach has been shown to damage the fibrillary structure of ECM,[42] and not removing all cell remnants, this method also allowed successful production of cell-derived ECMs on scaffolds and maintain most of the ECM components.[10,14,43] Along with these latter findings, we believe that the model of devitalized ECM presented here represents a simpler way to produce a matrix *in vitro* by using cost-effective freeze–thaw cycling, while still being able to accelerate and improve the osteogenic potential of MSCs as shown.

In summary, we produced an osteoblast-derived ECM by a simple devitalization treatment; this *in vitro* model of bone ECM improved the osteogenic potential of MSCs, reinforcing previous findings. This, combined with the increase in cell proliferation could be useful to expand autologous MSCs *ex vivo* and improve their use for bone regeneration.

A detailed proteomic analysis revealed known ECM components responsible for the observed effects and an overlap with the human bone microenvironment, but also novel ECM functions that need further investigation. Some candidate proteins could be overexpressed in ECM-secreting MSCs, to produce a tailor-made ECM that improves MSC properties to accelerate fracture healing, broadening the future applications of the cell-secreted ECM. In addition, MSCs could be isolated from patients to easily produce an autologous ECM, to improve patient-specific therapies. Overall, the devitalized ECM could be applied as natural biomaterial that mimics the osteogenic niche and to functionalize scaffolds to develop osteoinductive materials for the implanted cells *in vivo,* to robustly accelerate bone regeneration.

Acknowledgments

This work was supported by a grant from the Dutch government to the Netherlands Institute for Regenerative Medicine (NIRM, grant No: FES0908) and Erasmus Medical Center. The authors thank Molecular Medicine Post Graduated School, T. Strini, and C. S. van der Leije for technical assistance, P. Kumar for performing Western blots, Dr. L. Sasso, Dr. H. H Perez Garza, and Dr. M. K. Ghatkesar for helping with AFM and data interpretation, and K. Bezstarosti and D. Dekkers for MS analysis.

Authors' Contributions

M.B., B.E., R.A., J.P., and J.L. designed the research. M.B., S.C., E.R.T., I.E., Y.K., and M.K. performed the research. M.B., B.E., S.C., E.R.T., I.E., L.F.A., Y.K., M.K., J.D., J.P., and J.L. analyzed data. M.B., J.P., and J.L. drafted the article. M.B., B.E., J.P., R.A., and J.L. revised the final version of the article. All authors have approved the final article.

Disclosure Statement

No competing financial interest exist.

References

1. Caplan, A.I. Mesenchymal stem cells. J Orthop Res **9,** 641, 1991.
2. Pittenger, M.F., Mackay, A.M., Beck, S.C., *et al.* Multilineage potential of adult human mesenchymal stem cells. Science **284,** 143, 1999.
3. Caplan, A.I. Review. Mesenchymal stem cells: cell-based reconstructive therapy in orthopedics. Tissue Eng **11**, 1198, 2005.
4. Sommerfeldt, D.W., and Rubin, C.T. Biology of bone and how it orchestrates the form and function of the skeleton. Eur Spine J **10(Suppl. 2),** S86, 2001.
5. Alford, A.I., Kozloff, K.M., and Hankenson, K.D. Extracellular matrix networks in bone remodeling. Int J Biochem Cell Biol **65,** 20, 2015.
6. Hidalgo-Bastida, L.A., and Cartmell, S.H. Mesenchymal stem cells, osteoblasts and extracellular matrix proteins: enhancing cell adhesion and differentiation for bone tissue engineering. Tissue Eng B Rev **16,** 405, 2010.
7. Hynes, R.O. The extracellular matrix: not just pretty fibrils. Science **326,** 1216, 2009.
8. Guilak, F., Cohen, D.M., Estes, B.T., Gimble, J.M., Liedtke, W., and Chen, C.S. Control of stem cell fate by physical interactions with the extracellular matrix. Cell Stem Cell **5,** 17, 2009.
9. Badylak, S.F., Freytes, D.O., and Gilbert, T.W. Extracellular matrix as a biological scaffold material: structure and function. Acta Biomater **5,** 1, 2009.
10. Fitzpatrick, L.E., and McDevitt, T.C. Cell-derived matrices for tissue engineering and regenerative medicine applications. Biomater Sci **3,** 12, 2015.
11. Chen, X.D., Dusevich, V., Feng, J.Q., Manolagas, S.C., and Jilka, R.L. Extracellular matrix made by bone marrow cells facilitates expansion of marrow-derived mesenchymal progenitor cells and prevents their differentiation into osteoblasts. J Bone Miner Res **22,** 1943, 2007.
12. Lai, Y., Sun, Y., Skinner, C.M., *et al.* Reconstitution of marrow-derived extracellular matrix *ex vivo*: a robust culture system for expanding large-scale highly functional human mesenchymal stem cells. Stem Cells Dev **19,** 1095, 2010.
13. Sun, Y., Li, W., Lu, Z., *et al.* Rescuing replication and osteogenesis of aged mesenchymal stem cells by exposure to a young extracellular matrix. FASEB J **25,** 1474, 2011.
14. Datta, N., Holtorf, H.L., Sikavitsas, V.I., Jansen, J.A., and Mikos, A.G. Effect of bone extracellular matrix synthesized *in vitro* on the osteoblastic differentiation of marrow stromal cells. Biomaterials **26,** 971, 2005.
15. Mauney, J.R., Kaplan, D.L., and Volloch, V. Matrix-mediated retention of osteogenic differentiation potential by human adult bone marrow stromal cells during *ex vivo* expansion. Biomaterials **25,** 3233, 2004.
16. Prewitz, M.C., Seib, F.P., von Bonin, M., *et al.* Tightly anchored tissue-mimetic matrices as instructive stem cell microenvironments. Nat Methods **10,** 788, 2013.
17. Kolf, C.M., Song, L., Helm, J., and Tuan, R.S. Nascent osteoblast matrix inhibits osteogenesis of human mesenchymal stem cells *in vitro*. Stem Cell Res Ther **6,** 258, 2015.
18. Marinkovic, M., Block, T.J., Rakian, R., *et al.* One size does not fit all: developing a cell-specific niche for *in vitro* study of cell behavior. Matrix Biol **52–54,** 426, 2016.
19. Ragelle, H., Naba, A., Larson, B.L., *et al.* Comprehensive proteomic characterization of stem cell-derived extracellular matrices. Biomaterials **128,** 147, 2017.
20. Salasznyk, R.M., Williams, W.A., Boskey, A., Batorsky, A., and Plopper, G.E. Adhesion to vitronectin and collagen I promotes osteogenic differentiation of human mesenchymal stem cells. J Biomed Biotechnol **2004,** 24, 2004.
21. Santiago, J.A., Pogemiller, R., and Ogle, B.M. Heterogeneous differentiation of human mesenchymal stem cells in response to extended culture in extracellular matrices. Tissue Eng A **15,** 3911, 2009.
22. Ode, A., Duda, G.N., Glaeser, J.D., *et al.* Toward biomimetic materials in bone regeneration: functional behavior of mesenchymal stem cells on a broad spectrum of extracellular matrix components. J Biomed Mater Res A **95,** 1114, 2010.
23. Alves, R.D., Demmers, J.A., Bezstarosti, K., *et al.* Unraveling the human bone microenvironment beyond the classical extracellular matrix proteins: a human bone protein library. J Proteome Res **10,** 4725, 2011.
24. van Hengel, I.A.J., Riool, M., Fratila-Apachitei, L.E., *et al.* Selective laser melting porous metallic implants with immobilized silver nanoparticles kill and prevent biofilm formation by methicillin-resistant *Staphylococcus aureus*. Biomaterials **140,** 1, 2017.
25. Horzum, U., Ozdil, B., and Pesen-Okvur, D. Step-by-step quantitative analysis of focal adhesions. MethodsX **1,** 56, 2014.
26. Bruedigam, C., Driel, Mv, Koedam, M., *et al.* Basic techniques in human mesenchymal stem cell cultures: differentiation into osteogenic and adipogenic lineages, genetic perturbations, and phenotypic analyses. Curr Protoc Stem Cell Biol Chapter 1:p. Unit1H.3, 2011.
27. Abdallah, B.M., Ditzel, N., and Kassem, M. Assessment of bone formation capacity using *in vivo* transplantation assays: procedure and tissue analysis. Methods Mol Biol **455,** 89, 2008.
28. Morhayim, J., van de Peppel, J., Demmers, J.A., *et al.* Proteomic signatures of extracellular vesicles secreted by nonmineralizing and mineralizing human osteoblasts and stimulation of tumor cell growth. FASEB J **29,** 274, 2015.
29. Vizcaino, J.A., *et al.* Update of the PRIDE database and its related tools. Nucleic Acids Res **44,** 11033, 2016**.**
30. Huang da, W., Sherman, B.T., and Lempicki, R.A. Systematic and integrative analysis of large gene lists using David bioinformatics resources. Nat Protoc **4,** 44, 2009.
31. Alves, R.D., Eijken, M., Bezstarosti, K., Demmers, J.A., and van Leeuwen, J.P. Activin A suppresses osteoblast mineralization capacity by altering extracellular matrix (ECM) composition and impairing matrix vesicle (MV) production. Mol Cell Proteomics **12,** 2890, 2013.
32. Globus, R.K., Doty, S.B., Lull, J.C., Holmuhamedov, E., Humphries, M.J., and Damsky, C.H. Fibronectin is a

survival factor for differentiated osteoblasts. J Cell Sci **111(Pt 10),** 1385, 1998.
33. Mackie, E.J., Abraham, L.A., Taylor, S.L., Tucker, R.P., and Murphy, L.I. Regulation of tenascin-C expression in bone cells by transforming growth factor-beta. Bone **22,** 301, 1998.
34. Delany, A.M., Kalajzic, I., Bradshaw, A.D., Sage, E.H., and Canalis, E. Osteonectin-null mutation compromises osteoblast formation, maturation, and survival. Endocrinology **144,** 2588, 2003.
35. Anderson, H.C., Garimella, R., and Tague, S.E. The role of matrix vesicles in growth plate development and biomineralization. Front Biosci **10,** 822, 2005.
36. Schafer, C., Heiss, A., Schwarz, A., *et al.* The serum protein alpha 2-Heremans-Schmid glycoprotein/fetuin-A is a systemically acting inhibitor of ectopic calcification. J Clin Invest **112,** 357, 2003.
37. Karsdal, M.A., Larsen, L., Engsig, M.T., *et al.* Matrix metalloproteinase-dependent activation of latent transforming growth factor-beta controls the conversion of osteoblasts into osteocytes by blocking osteoblast apoptosis. J Biol Chem **277,** 44061, 2002.
38. Danjo, A., Yamaza, T., Kido, M.A., *et al.* Cystatin C stimulates the differentiation of mouse osteoblastic cells and bone formation. Biochem Biophys Res Commun **360,** 199, 2007.
39. Sinder, B.P., Pettit, A.R., and McCauley, L.K. Macrophages: their emerging roles in bone. J Bone Miner Res **30,** 2140, 2015.
40. Klein, G., Beck, S., and Muller, C.A. Tenascin is a cytoadhesive extracellular matrix component of the human hematopoietic microenvironment. J Cell Biol **123,** 1027, 1993.
41. Wang, Z., and Chesler, N.C. Role of collagen content and cross-linking in large pulmonary arterial stiffening after chronic hypoxia. Biomech Model Mechanobiol **11,** 279, 2012.
42. Tour, G., Wendel, M., and Tcacencu, I. Cell-derived matrix enhances osteogenic properties of hydroxyapatite. Tissue Eng A **17,** 127, 2011.
43. Thibault, R.A., Scott Baggett, L., Mikos, A.G., and Kasper, F.K. Osteogenic differentiation of mesenchymal stem cells on pregenerated extracellular matrix scaffolds in the absence of osteogenic cell culture supplements. Tissue Eng A **16,** 431, 2010.

Address correspondence to:
Marta Baroncelli, MSc
Department of Internal Medicine
Erasmus University Medical Center
Wytemaweg 80
Rotterdam 3015 CN
The Netherlands

E-mail: martabaroncelli@yahoo.it

Received: October 24, 2017
Accepted: March 19, 2018
Online Publication Date: May 17, 2018